IMAGE INTERPRETABILITY CHARACTERIZATION OF THEOS PANCHROMATIC IMAGING SYSTEM

Suphongsa Khetkeeree[1], Sompong Liangrocapart[1] and Panatda Kiatlertseree[2]
[1]Mahanakorn University of Technology, 140 Cheumsampan Rd, Nongchock, Bangkok, Thailand,
Email: suphongs@mut.ac.th, sompong@mut.ac.th
[2] Geo-Informatics & Space Technology Development Agency (Public Organization),
88 Thung Sukala, Siracha, Chonburi, Thailand,
Email: panatda@gistda.or.th

KEYWORDS: NIIRS, GIQE, image quality, THEOS

ABSTRACT: In this paper, we present the image interpretability characterization of Thailand Earth Observation System (THEOS) panchromatic imaging system with National Imagery Interpretability Rating Scale (NIIRS). The NIIRS is widely used for overall image quality assessment in the remote sensing field. We estimate the NIIRS by employing the General Image Quality Equation (GIQE) version 4. This GIQE is composed of many spatial characteristics such as Relative Edge Response (RER), Ground Sample Distance (GSD), Signal to Noise Ratio (SNR) and edge overshoot. A hyperbolic tangent function is proposed in this work to construct a step edge profile. This function shows an excellent correlation to step edge response and can be used to estimate the RER and edge overshoot. NIIRS of THEOS panchromatic system is derived from the level-1A data product from 2009 to 2015. The experimental results show a slight change of the RER, H and NIIRS. The SNR also decreases, but it is an insignificant effect for the NIIRS estimation. The average NIIRS of THEOS level-1A panchromatic imaging system is about 3.42. This proves that THEOS panchromatic system is still in an excellent condition after 8 years in operation.

1. INTRODUCTION

Thailand Earth Observation System (THEOS) is high-resolution observation satellite that launched in 2008. It has two push-broom scanning optical instrument, i.e. panchromatic and multispectral cameras. The panchromatic camera has high spatial resolution (2m) and the multispectral camera (blue green red and Near IR) has large swath (90km) with 15m-spatial resolution. In the past, Modulation Transfer Function (MTF) was evaluated to indicate the quality of the imaging system. However, it cannot completely describe the overall image quality. National Imagery Interpretability Rating Scale (NIIRS) is an alternative choice for indicating image quality. This scale was developed by the Imagery Resolution Assessments and Reporting Standards (IRARS, 2016) to evaluate the overall image quality that corresponding to the view of human observers. The NIIRS is a 10-level scale (0 to 9) of image interpretability. Each level is defined by a series of interpretation task (Leachtenauer et al., 1997). However, the NIIRS may be estimated from General Image Quality Equation (GIQE). The GIQE is an empirical formula that uses many image characteristics such as Relative Edge Response (RER), Ground Sample Distance (GSD), Signal to Noise Ratio (SNR) and edge overshoot. In this paper, the THEOS panchromatic images from 2009 to 2015 are used to evaluate the NIIRS of THEOS panchromatic imaging system.

2. NATIONAL IMAGERY INTERPRETABILITY RATING SCALE

Leachtenauer et al. developed the GIQE for NIIRS estimation. This GIQE is version 4 that popular use of the remote sensing filed (Li et al., 2014, Kim et al., 2008, Ryan et al., 2003). The equation can be written as below equation.

$$\mathrm{NIIRS} = 10.251 - a\log_{10}\mathrm{GSD_{GM}} + b\log_{10}\mathrm{RER_{GM}} - 0.656\mathrm{H} - 0.344\mathrm{G/SNR} \quad (1)$$

Where $\mathrm{GSD_{GM}}$ is a geometric mean of Ground Sampling Distance (GSD) that computes in inch unit, $\mathrm{RER_{GM}}$ is a geometric mean of Relative Edge Response (RER), H is an edge overshoot, G is the noise gain of the MTF compensation kernel and SNR is the signal to noise ratio. The constants a and b are equal 3.32 and 1.559, respectively, if $\mathrm{RER_{GM}} \geq 0.9$, and they are equal 3.16 and 2.817, respectively, if $\mathrm{RER_{GM}} < 0.9$. The GIQE v.4 is validated over the range that listed in Table 1. THEOS panchromatic system can be applied to evaluate the NIIRS by this GIQE because its official GSD is about 2.0 m.

Table 1. The validation limit of GIQE v.4

	minimum	maximum
GSD	3 in. or 0.076 m	80 in. or 2.032 m
RER	0.2	1.3
G	1	19
SNR	2	130
H	0.9	1.9

2.1 Ground Sample Distance

The GSD of THEOS satellite in each scene may be different because the optical instruments have an off-nadir imaging mode and the attitude of this satellite can be changed. The meta data of THEOS images given the attitude level and angle of point view that is the angle of along track and across track. Hence, the formula for calculating the exact GSD of each scene can be written as follows.

$$\mathrm{GSD} = \frac{p}{f} \cdot \frac{h}{\cos^2 \theta} \tag{2}$$

Where p is a pixel pith, f is a focal length, h is an attitude level of satellite and θ is an off-nadir angle. In this GIQE, the GSD is computed in both across track (x) and along track (y) in inches while a geometric mean of GSD can compute as equation (3).

$$\mathrm{GSD}_{\mathrm{GM}} = \sqrt{\mathrm{GSD}_{\mathrm{x}} \cdot \mathrm{GSD}_{\mathrm{y}}} \tag{3}$$

2.2 Relative Edge Response and Edge Overshoot

The step edge image is used to construct the edge response (ER) profile. For RER and H calculation, we can compute them from normalized edge response as

$$\mathrm{RER} = \mathrm{ER}(0.5p) - \mathrm{ER}(-0.5p) \tag{4}$$

where 0.5p is a haft of a pixel and H is the maximum value over 1.0-3.0 pixels from the edge location. However, if ER is monotonic increase, H can determine at 1.25 pixels from the edge. The estimation of H for each case can be shown in Figure 1.

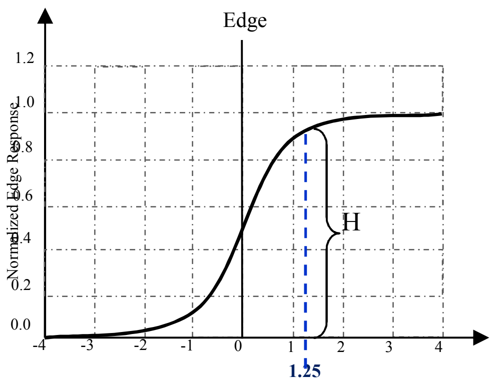

(a)

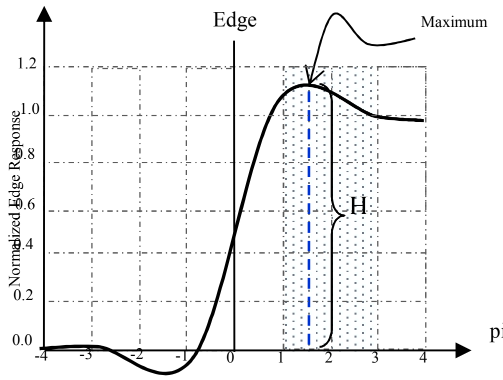

(b)

Figure 1. The definition of edge overshoot for GIQEv.4, (a) the edge response is monotonic increase and (b) the edge ringing is occurred.

2.3 Signal to Noise Ratio and Noise Gain

The SNR is estimated from differential radiance levels of Lambertian scene at 7% and 15% of reflectance (Ryan et al., 2003). However, this method can complicate to estimation and SNR has least effect on the NIIRS values (Li et al., 2014), (GSD 72%, RER20%, and SNR < 1%) (Bai, 2010). In this paper, we use a laboratory method for estimating the SNR. It can write in the form of a ratio of mean values (μ) and standard deviation (σ) in homogeneous area. That is

$$\mathrm{SNR} = \frac{\mu}{\sigma} \tag{5}$$

A parameter G is the noise gain which is the root mean square of a filter that uses to compensate the MTF. The mathematical formula of noise gain can write as

$$G = \sqrt{\sum_{i=1}^{M}\sum_{j=1}^{N}\left(K_{ij}\right)^2} \tag{6}$$

where K is MTF compensated filter. However, if image is not compensated, we can define G as 1.

3. THEOS IMAGE ANALYSIS

3.1 Area Selection

A target for estimating the NIIRS must be the step edge to construct the ER. We use the target for the remote sensing calibration which has been located in the airport at Salon de Provence, France. This target is 60m$\times$ 60m chess board and its inclination angle is 98.7^{o}. For THEOS satellite, the pattern orientation angle with to CCD line is about 14^{o} (Natpramoon et al., 2007). Six different area are selected as Figure 2. Region 1-2 and 3-4 are used to estimate across ER and along ER, respectively, while region 5-6 are employed to estimate the SNR.

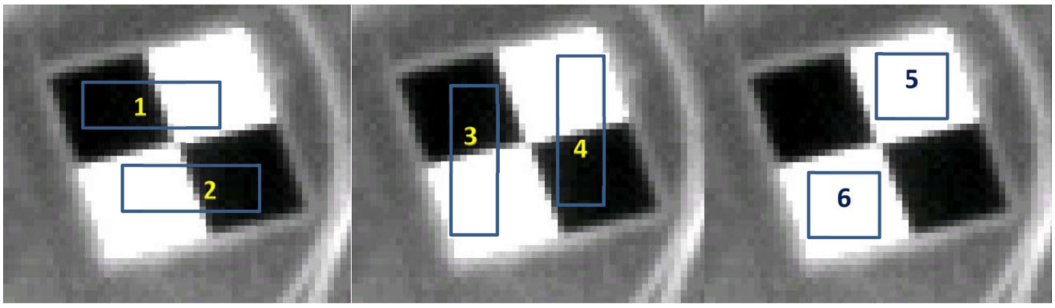

Figure 2. The regions of interest for estimating the ER and SNR

3.2 Edge Response Construction

The slanted edge method (Turkmenoglu and Yaghoglu, 2013) is used to estimating the ER. A subpixel edge location in region of interest is determined as primary process. The gradient image of each region is fitted by second order polynomial. Edge location is calculated by using the mathematics of maximum point definition. After that, the linear regression is employed for adjusting the edge location, because we assume the edge orientation is a straight line. The superposition of each profile by fixing the subpixel edge location produce the over sampling data of edge response. The shape of this oversampling data is similar sigmoid function which shows in Figure 3(a). Therefore, we employ a tangent hyperbolic function to fit the edge profile because it is simplicity, convenience and useful for constructing the edge response function. The general form of a tangent hyperbolic function is shown in equation (7).

$$\mathrm{y} = A\tanh\left(\frac{x-C}{B}\right)+D \tag{7}$$

Where A is a difference of a mean pixel value in bright and dark, B is parameter for adjusting the slope of this function, C is edge location and D is offset. In this case, the edge location is fixed at zero, so C=0. Let U is the mean DN (digital number) of bright and L is the mean DN (digital number) of dark. We can estimate the A and D as follows.

$$A = \frac{\mathrm{U} - \mathrm{L}}{2} \text{ and } D = \frac{\mathrm{U} + \mathrm{L}}{2} \tag{8}$$

while parameter B can be estimated from equation (9).

$$B = \arg\min_{B} \left[\sum_{i=1}^{N} \left\| \hat{y}_i - y_i \right\|^2 \right] \tag{9}$$

Where $\hat{y}_i$ is a DN of the edge profile data and y_i is a value of a tangent hyperbolic function at i's position. The curve of a tangent hyperbolic function that fit on an oversampling data is shown on the Figure 3(a). The Figure 3(b) is a normalization of the tangent hyperbolic at pixel position.

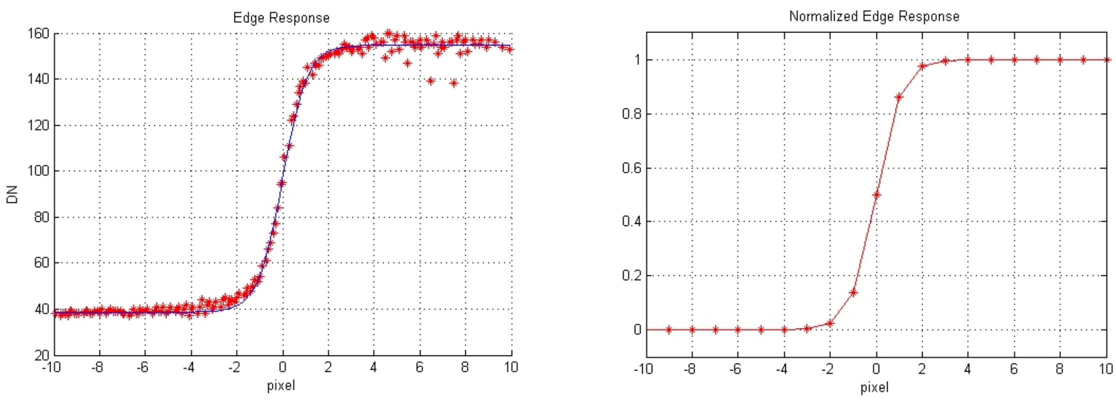

(a) (b)

Figure 3. The edge profiles data before MTF compensation a) a fine tangent hyperbolic function that fit on all edge profile data and b) Normalized edge response

The formula of normalized edge response and the RER in the tangent hyperbolic form can be written as below.

$$\mathrm{ER} = 0.5 \tanh\left(\frac{x}{B} \right) + 0.5 \tag{10}$$

$$\mathrm{RER} = 0.5(\tanh(\frac{0.5}{B}) - \tanh(-\frac{0.5}{B})) \tag{11}$$

The geometric mean of RER and H are similar computed as the GSD, that is $\mathrm{RER}_{\mathrm{GM}} = \sqrt{\mathrm{RER}_{\mathrm{x}} \cdot \mathrm{RER}_{\mathrm{y}}}$ and $\mathrm{H}_{\mathrm{GM}} = \sqrt{\mathrm{H}_{\mathrm{x}} \cdot \mathrm{H}_{\mathrm{y}}}$.

The edge profile after the MTF compensation often occurs the ringing that is a cause of an edge overshoot in the edge profile (Figure 4). The tangent hyperbolic cannot directly estimate the edge overshoot, but the parameters A and D in the general form of tangent hyperbolic can use to normalize the edge response which the edge overshoot is not disappearing.

The normalized oversampling data of this case is fit by a third order polynomial on over -3 to 3 pixels to estimate the height of edge overshoot. Figure 4 show the edge response in the MTF compensation case, the dash line is the tangent hyperbolic fit which helps to normalizing the prior data and the continuous line represents the third order polynomial fit on over -3 to 3 which this interval often has the edge ringing. We use the maximum value of the third order polynomial to define the edge overshoot height.

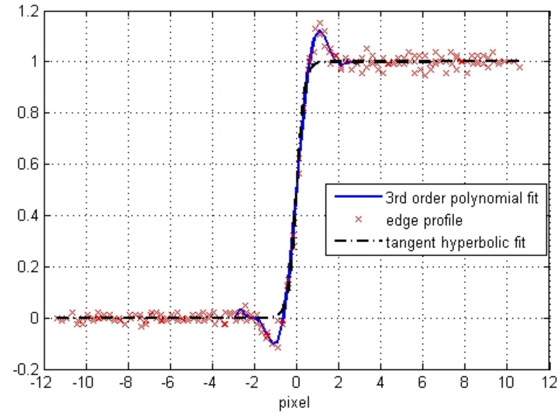

Figure 4. The edge profiles data after MTF compensation, a third order polynomial fit for estimating the edge overshoot and a normalized tangent hyperbolic for estimating the RER.

4. EXPERIMANTAL RESULTS AND DISCUSSION

The level-1A THEOS images at Salon de Provence, France, since 2008 to 2015 are estimated the NIIRS. The experimental results of GSD, RER, H, G, SNR and NIIRS calculation can show in table 2. The results show a little change of RER, H and NIIRS over 8 years. That is the overall image quality is stable. However, the tendency of the SNR is increasing, but it less effect to the NIIRS estimation.

Table 2. The experimental results of GSD, RER, H, G, SNR and NIIRS for level -1A images

Date	GSD_{GM} (m)	RER_{GM}	H_{GM}	G	SNR	NIIRS
24-JUN-2009	1.869	0.843	1.086	2.57	70	**3.42**
20-JUL-2009	1.874	0.846	1.094	2.57	60	**3.41**
15-AUG-2009	1.870	0.849	1.088	2.57	70	**3.42**
6-MAR-2010	1.873	0.850	1.081	2.57	51	**3.42**
23-JUN-2010	1.870	0.845	1.083	2.57	65	**3.42**
14-JUL-2010	1.873	0.842	1.086	2.57	58	**3.41**
8-MAR-2012	1.870	0.846	1.082	2.57	58	**3.42**
29-MAR-2012	1.882	0.844	1.080	2.57	51	**3.41**
25-MAY-2012	1.870	0.852	1.080	2.57	58	**3.43**
9-FEB-2013	1.870	0.850	1.079	2.57	45	**3.42**
10-JUL-2013	1.875	0.852	1.091	2.57	49	**3.42**
22-NOV-2013	1.870	0.840	1.078	2.57	37	**3.41**
6-MAR-2014	1.870	0.849	1.080	2.57	51	**3.43**
6-APR-2014	1.874	0.844	1.074	2.57	51	**3.42**
31-OCT-2014	1.873	0.851	1.071	2.57	38	**3.43**
2-FEB-2015	1.880	0.845	1.074	2.57	37	**3.41**
28-FEB-2015	1.881	0.849	1.080	2.57	42	**3.41**
22-MAY-2015	1.869	0.841	1.069	2.57	38	**3.42**
17-JUN-2015	1.871	0.832	1.068	2.57	42	**3.40**
8-JUL-2015	1.883	0.830	1.074	2.57	40	**3.39**
18-JUL-2015	1.874	0.836	1.071	2.57	43	**3.41**
MEAN	**1.873**	**0.844**	**1.079**	**2.57**	**50**	**3.42**

For accuracy of this estimate, we compare the NIIRS with another high spatial resolution satellite, i.e. IKONOS(Ryan, 2003), QuickBird(Li, 2014), Ziyuan-3 (Li, 2014), SPOT5(Li, 2014). Figure 5 shows the NIIRS comparison with the GSD of each satellite. The official GSD of THEOS panchromatic imaging system is near the GSD of Ziyuan-3 panchromatic imaging system, but the NIIRS of THEOS is more better than Ziyuan-3. Because the true GSD of THEOS is lower than official design (GSD of official design is 2.0 m , while true GSD is about 1.87 m).

The other approach to prove the NIIRS accuracy, we use the criteria of NIIRS. For NIIRS rating 3.3, the image can detect individual large buildings (e.g., house, barn) in a farmstead. The THEOS level-1A panchromatic imagery can detect an individual house in a farmstead as the Figure 6 (a). For the criteria of NIIRS 3.4, it can distinguish between crop lands and pasture land which the images from THEOS imaging can show as the Figure 6 (b).

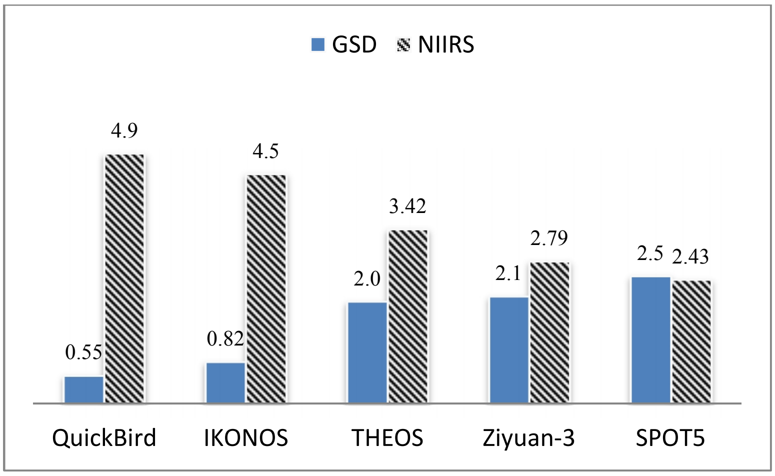

Figure 5. Comparison of the THEOS panchromatic GSD and NIIRS with another high resolution satellite

(a) (b)

Figure 6. Stretching images that show information of criteria, (a) an individual house in the farm and (b) an image can distinguish between cropland and pasture land.

5. CONCLUSION

This paper estimates the NIIRS of level-1A panchromatic THEOS imaging system by using GIQE v.4. Twenty-one images of a test-site target at Salon de Provence, France, have been taken from 2009 to 2015. These images are used here for estimating the NIIRS. The slant edge method is applied for constructing the edge response. The tangent hyperbolic function is employed for fitting the curve of edge response. The experimental results show a slight change of the RER, H and NIIRS. The SNR also decreases, but it is an insignificant effect for the NIIRS estimation. The average NIIRS of THEOS level-1A panchromatic imaging system is about 3.42. This value is also compared to other similar spatial resolution range, i.e. IKONOS, QuickBird, Ziyuan-3 and SPOT-5. Slight change in NIIRS shows that THEOS panchromatic system is still in an excellent condition over 8 years in operation.

6. REFERENCES

Bai, H.G., 2010. Research on Image Quality Estimation and Evaluation Methods of Remote Sensing Based on NIIRS. Master's Thesis, Xidian University, Xian, Shaanxi, China.

Imagery Resolution Assessment and Reporting Standards (IRARS) Committee., 2016. Civil NIIRS Reference Guide. Retrieved August 16, 2016, from: http://fas.org/irp/imint/niirs_c /app2.htm

Kim, T., Kim, H. and Kim, H.S., 2008. Image-base estimation and validation of NIIRS for high-resolution satellite images. The International Archives of the Photogrammetry, Remote Sensing and Spatial Information Sciences, Beijing 2008.

Leachtenauer, C.J., Malila, W., Irvine, J., Colburn, L. and Salvaggio, N., 1997. General image-quality equation: GIQE. Applied Optics, vol. 36, pp. 8322-8328.

Li, L., Luo, H., and Zhu, H., 2014. Estimation of the interpretability of ZY-3 sensor corrected panchromatic nadir data**.** Remote Sense, vol.6, pp. 4409-4429.

Nutpramoon, R., Weerawong, K., and Apaphant, P., 2007. In-orbit MTF measurement for THEOS imaging system. Proceeding at Asian conference on remote sensing 2007, Kuala Lumpur, Philippines.

Ryan, R., Baldridge, B., Schowengerdt, R.A., Choi, T., Helder, D.L. and Blonski, S., 2003. IKONOS spatial resolution and image interpretability characterization. Remote sensing of environment, vol.88, pp. 37-52.

Turkmenoglu, M., and Yaglioglu, B., 2013. On-orbit modulation transfer function estimation for RASAT. 6th International conference on Recent Advances in Space Technologies (RAST).